

Candidate Elastic Quantum Critical Point in $\text{LaCu}_{6-x}\text{Au}_x$

L. Poudel,^{1,2,*} A. F. May,³ M. R. Koehler,⁴ M. A. McGuire,³ S. Mukhopadhyay,³ S. Calder,² R. E. Baumbach,⁵ R. Mukherjee,⁴ D. Sapkota,¹ C. de la Cruz,² D. J. Singh,⁶ D. Mandrus,^{1,4,3} and A. D. Christianson^{2,1}

¹Department of Physics & Astronomy, University of Tennessee, Knoxville, Tennessee 37966, USA

²Quantum Condensed Matter Division, Oak Ridge National Laboratory, Oak Ridge, Tennessee 37831, USA

³Materials Science & Technology Division, Oak Ridge National Laboratory, Oak Ridge, Tennessee 37831, USA

⁴Department of Material Science & Engineering, University of Tennessee, Knoxville, Tennessee 37966, USA

⁵National High Magnetic Field Laboratory, Florida State University, Tallahassee, Florida 32306, USA

⁶Department of Physics & Astronomy, University of Missouri, Columbia, Missouri 65211, USA

(Received 4 August 2016; revised manuscript received 28 October 2016; published 30 November 2016)

The structural properties of $\text{LaCu}_{6-x}\text{Au}_x$ are studied using neutron diffraction, x-ray diffraction, and heat capacity measurements. The continuous orthorhombic-monoclinic structural phase transition in LaCu_6 is suppressed linearly with Au substitution until a complete suppression of the structural phase transition occurs at the critical composition $x_c = 0.3$. Heat capacity measurements at low temperatures indicate residual structural instability at x_c . The instability is ferroelastic in nature, with density functional theory calculations showing negligible coupling to electronic states near the Fermi level. The data and calculations presented here are consistent with the zero temperature termination of a continuous structural phase transition suggesting that the $\text{LaCu}_{6-x}\text{Au}_x$ series hosts an elastic quantum critical point.

DOI: 10.1103/PhysRevLett.117.235701

Quantum fluctuations in the vicinity of a quantum critical point (QCP) generate a seemingly inexhaustible supply of new phases of matter [1–9]. Although of great interest, the competing phases typically found near a QCP obscure the fundamental critical behavior and consequently a general understanding of such phase transitions has remained elusive and no concept as powerful as the universality of classical continuous phase transitions has emerged. Hence, new examples of QCPs are highly prized as a means of probing the general organizing principles of QCPs. Thus, it is rather surprising, given the immense body of work devoted to the study of structural phase transitions, that little attention has been given to the concept of a structural quantum critical point (SQCP). The bulk of previous work on QCPs involving structural degrees of freedom has been focused on an incipient ferroelectric state [10–16]. For example, the quantum zero point motion in SrTiO_3 acts to prevent the complete softening of the relevant optic phonon mode resulting in a quantum paraelectric on the verge of ferroelectricity [17,18].

Recently, interest in SQCPs has risen. For instance, ScF_3 has been discussed as an example of a SQCP in an ionic insulator [19]. On the other hand, in metallic systems, there have been several studies of a family of Rameika phase stannides where a structural phase transition with concomitant changes in the Fermi surface can be tuned to a SQCP [20–26]. Here, we approach the problem of a SQCP from the perspective of a structural phase transition where elastic instabilities are primarily responsible for the lowering of symmetry and electronic degrees of freedom are unimportant. This type of transition is similar to the nematic

transition as found in the Fe-based superconductors [27–29] where the point group symmetry is lowered without a change in translational symmetry. The two cases are nevertheless distinct, as the nematic transition in Fe-based superconductors is strongly coupled to electronic degrees of freedom, whereas the elastic transition studied here is in the opposite decoupled limit.

Elastic QCPs, where the quantum zero point motion of the atoms destroys an elastically ordered state, have been the subject of recent theoretical study [30]. However, examples where electronic degrees of freedom are uninvolved have, to the best of our knowledge, eluded study thus far. To remedy this, we have identified the $\text{LaCu}_{6-x}\text{Au}_x$ series as a promising candidate to host an elastic QCP. LaCu_6 exhibits a continuous phase transition from an orthorhombic ($Pnma$) to a monoclinic ($P2_1/c$) crystal structure at 460 K [31]. A phase transition of this type is a common feature of the RCu_6 ($R = \text{La, Ce, Pr, Nd, Sm}$) family including the $\text{CeCu}_{6-x}\text{Au}_x$ series, which hosts one of the most studied antiferromagnetic QCPs [4,31–38]. The continuous nature of the orthorhombic-monoclinic phase transition is evidenced by a smooth evolution of the monoclinic distortion [32,33], a gradual softening of the C_{66} elastic constant [34], a progressive softening of a transverse acoustic phonon mode [31], and a continuous change in the linear thermal expansion coefficient [35]. Furthermore, no signature of the structural phase transition is visible in resistivity measurements [39], suggesting that the electronic degrees of freedom are of little consequence. Finally, the absence of f electrons in LaCu_6 eliminates complications due to a magnetic ground state.

In this Letter, we present a detailed study of the structural properties of the $\text{LaCu}_{6-x}\text{Au}_x$ series. The structural transition temperature T_S in $\text{LaCu}_{6-x}\text{Au}_x$ decreases linearly with Au doping until the critical composition $x_c = 0.3$. The low temperature heat capacity is maximum at x_c as is typical for a QCP. Density-functional theory (DFT) calculations show that the Fermi surface is essentially unchanged at T_S and that the structural transition occurs as the result of a zone center elastic instability. The measurements taken together with the calculations point towards an elastic QCP in the $\text{LaCu}_{6-x}\text{Au}_x$ series.

Polycrystalline samples of $\text{LaCu}_{6-x}\text{Au}_x$ were prepared by arc melting stoichiometric compositions of La (purity $\geq 99.998\%$, Ames laboratory), Cu (purity 99.9999%, Alpha Aesar), and Au (purity 99.9999%, Alpha Aesar). Specific heat measurements were performed on selected compositions. Structural properties for each composition were obtained from a Rietveld analysis of neutron and/or x-ray diffraction patterns. Further details of sample characterization are provided in Supplemental Material [40]. The lattice parameters transform from orthorhombic to monoclinic symmetry as $a \rightarrow c_m$, $b \rightarrow a_m$, $c \rightarrow b_m$, and β_m denotes the monoclinic angle.

The structural phase transition in LaCu_6 was tuned by substituting Cu by isoelectronic Au, which results in an overall expansion of the unit cell due to the larger atomic radius of Au [35]. With Au substitution for $x \leq 0.7$, the lattice parameters a and c increase whereas b decreases [40]. For each composition studied, the lattice parameters increase smoothly with temperature and no discontinuities were observed at T_S [40]. Additional information is provided by high resolution synchrotron x-ray measurements of LaCu_6 (monoclinic) and $\text{LaCu}_{5.7}\text{Au}_{0.3}$ (orthorhombic) [40]. In the orthorhombic structure, La occupies a $4c$ site, whereas the Cu atoms are distributed among one $8d$ and four $4c$ sites. The Au atoms in $\text{LaCu}_{5.7}\text{Au}_{0.3}$ occupy only a particular $4c$ site: Cu2 (0.146, 0.25, 0.139). A similar site preference was also observed in $\text{CeCu}_{6-x}\text{Au}_x$ [45] and $\text{CeCu}_{6-x}\text{Ag}_x$ [46] and is due to the large volume of the Cu2 site [35]. At the structural transition, the symmetry of all $4c$ sites remains unchanged, whereas the orthorhombic $8d$ site separates into two monoclinic $4c$ sites due to the loss of the mirror symmetry along the (100) plane.

The monoclinic distortion results in the splitting of Bragg peaks as shown in Fig. 1(a). The shear strain $e_{13} = \frac{1}{2}(c_m/c_o) \cos \beta_m$ (see Ref. [47] and Fig. S2 [40]) acts as an order parameter for the phase transition. c_0 is the extrapolation of the lattice parameter from the orthorhombic phase into the monoclinic phase. Hence, to determine T_S for each composition, the values of $\cos^2 \beta_m$ were extrapolated as a function of temperature [Fig. 1(b)]. The resulting transition temperatures in $\text{LaCu}_{6-x}\text{Au}_x$ are summarized in Fig. 2. A linear decrease in T_S with Au composition is observed. Extrapolation of T_S as a function of Au composition shows that the phase transition disappears at $x_c = 0.30(3)$ [48].

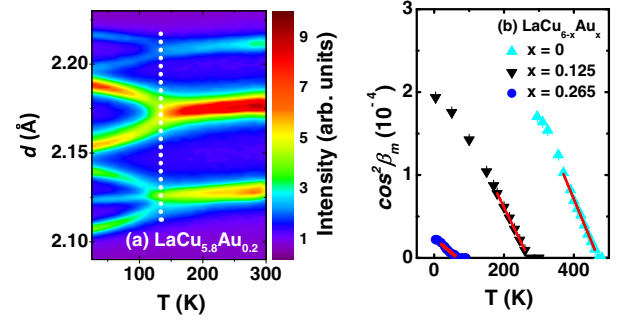


FIG. 1. (a) X-ray diffraction data showing the splitting of selected Bragg peaks at T_S in $\text{LaCu}_{5.8}\text{Au}_{0.2}$. The following indexing scheme describes the splitting of the peaks: $(122) \rightarrow (22 \pm 1)$, $(220) \rightarrow (20 \pm 2)$, $(221) \rightarrow (21 \pm 2)$. The peak between (21 ± 2) is the orthorhombic (303) reflection, which becomes the monoclinic (033) reflection. The vertical dotted line indicates the temperature where the peaks begin to separate. Each pixel represents a triangulation-based linear interpolation of the measurement performed with 10 K steps in temperature. (b) The temperature dependence of $\cos^2 \beta_m$ in $\text{LaCu}_{6-x}\text{Au}_x$ determined from neutron diffraction data. $\cos^2 \beta_m$ varies smoothly near T_S . T_S was estimated from a linear extrapolation (red line) of $\cos^2 \beta_m$.

A similar value of x_c is provided by the extrapolation of $\cos^2 \beta_m$ at 20 K for each composition [40].

First principle calculations provide additional insight into the nature of the structural phase transition in $\text{LaCu}_{6-x}\text{Au}_x$. DFT calculations using the Perdew-Burke-Enzerhof generalized gradient approximation [49] were performed for LaCu_6 with experimental structures. Phonon calculations were performed with the Phonopy code [50]

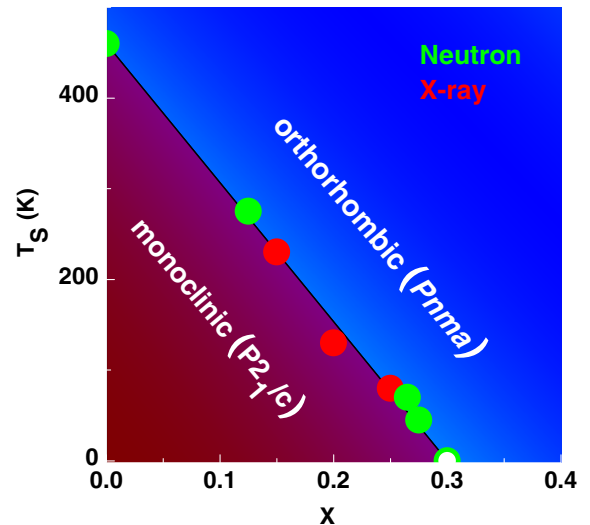


FIG. 2. Structural phase diagram of $\text{LaCu}_{6-x}\text{Au}_x$. The open circle represents the point where no structural phase transition is observed above 2 K. The statistical error bars for T_S are smaller than the symbol size. A linear extrapolation of T_S with temperature indicates $x_c = 0.3$.

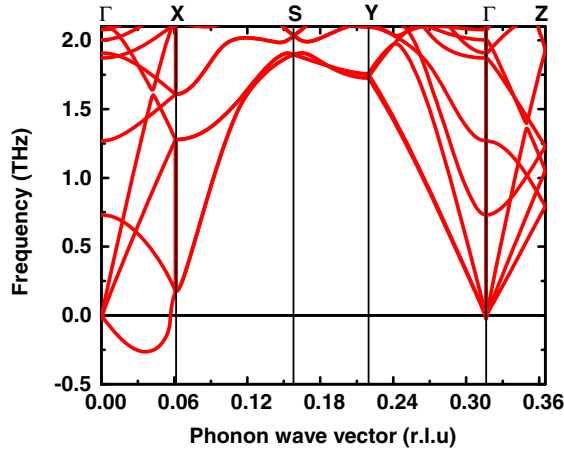


FIG. 3. Calculated phonon dispersions of LaCu_6 with the $Pnma$ crystal structure. The imaginary phonon mode frequency from Γ to X indicates the instability of the orthorhombic structure.

based on underlying DFT calculations by the VASP code [51,52]. Electronic structure calculations were performed with the general potential linearized augmented plane wave (LAPW) method [52] using well converged basis sets as implemented in WIEN2k [53,54] where LAPW plus local orbital basis sets were used with LAPW sphere radii of 2.3 (2.25) bohr for La (Cu) in both orthorhombic and monoclinic cells. The internal atomic coordinates were fully relaxed with lattice parameters fixed to experimental values. All calculations were for $T = 0$ K.

The phonon dispersions for the orthorhombic structure (Fig. 3) show a clear instability of ferroelastic character whereas phonon calculations for the monoclinic phase [40] find only stable modes consistent with the fact that this is the ground state structure. Figure 3 shows the unstable transverse acoustic branch is found along $\Gamma - X$. This branch has an upward curvature, meaning that the instability is a zone center elastic instability. There are no soft optic phonons. Such a zone center symmetry lowering without other long range orders can reflect nematicity, associated with orbital or magnetic degrees of freedom as has been suggested in the Fe-based superconductors [27–29], Pomeranchuk instabilities [55], or lattice instability due to steric effects, i.e., underbonding or poor matches between ion sizes and the lattice structure. Our electronic structure calculations indicate that the latter is the case in LaCu_6 . The phonon softening calculated by DFT is in line with that observed in CeCu_6 and LaCu_6 [31]. The transition is continuous and originates from a zone center elastic instability, and may thus be termed ferroelastic, although we have not observed switching in the low- T phase and therefore formally it is coelastic [56].

The electronic densities of states are very similar for the monoclinic and orthorhombic phases. In particular, there is no significant change around the Fermi level E_F [40]. Similar to prior calculations [57], the Cu d bands are occupied and are located from approximately -5 to

-1.7 eV with respect to E_F and therefore do not play a role in the low energy physics, which instead depends on an electronic structure derived mainly from Cu and La s states. The Fermi surface is derived from five bands that cross E_F and is similar in both of the two phases [40]. The Fermi level density of states is very similar between the two phases: $N(E_F) = 3.52 \text{ eV}^{-1}$ (3.37 eV^{-1}) per formula unit for the orthorhombic (monoclinic) phase.

As noted above, another possible driver for a symmetry lowering is a Pomeranchuk instability of the Fermi surface [55]. Such a scenario would involve a strong reconstruction of the Fermi surface, as in the Fe-based superconductors at the nematic transition [58]. We calculated transport coefficients using the BoltzTraPCode [59] and find very weak monoclinicity of these in the low temperature phase. In particular, the off-diagonal monoclinic component of the conductivity tensor with constant scattering time is 4.8% of the average diagonal component, while the density of states is hardly changed, and experimental evidence does not suggest sizable Fermi surface reconstruction.

These results imply that the phase transition is not driven electronically, e.g., by an instability of the Fermi surface such as a density wave, as there is no substantial reconstruction of the electronic structure associated with the transition. A further implication is that the structural transition does not couple strongly to electrons at the Fermi energy, meaning that only weak effects in transport and other electronic properties may be expected. Together, the unstable transverse acoustic branch along $\Gamma - X$ and the decoupled electronic degrees of freedom are consistent with a ferroelastic ground state in LaCu_6 . We note that the variations of the transition temperature upon substitution on the La and Cu site are consistent with the characterization of the transition as a ferroelastic transition driven by size effects; specifically, substitution of a larger atom on the Cu site behaves similarly to the substitution of a smaller atom on the La site [35], making a connection between the instability and size mismatch, as opposed to chemical pressure, bandwidth, etc.

Having determined the structural transition is elastic in origin and the electronic degrees of freedom are unimportant, we now examine the quantum critical fluctuations through studies of the thermodynamic properties with heat capacity measurements. Typically, at a QCP, an energy scale associated with the critical fluctuations vanishes resulting in an enhanced heat capacity as the QCP is approached. In the case of an elastic QCP, the quantum critical fluctuations drive critical dynamics, which are reflected in the softening of the transverse acoustic mode discussed above. Further insight into the quantum critical fluctuations is provided by the theoretical work of Ref. [30], which predicts that the quantum fluctuations enhance the heat capacity and drive a departure from Debye's law. As will be described below, an enhanced

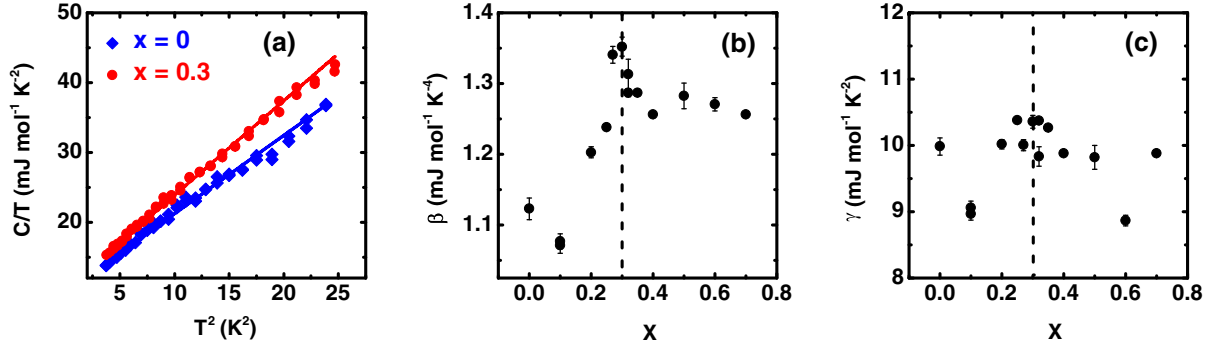


FIG. 4. (a) Heat capacity data showing T^3 behavior at low temperature for LaCu_6 ($x = 0$) and $\text{LaCu}_{5.7}\text{Au}_{0.3}$ ($x_c = 0.3$). The solid lines are a fit to the data of the form $C = \gamma T + \beta T^3$. (b),(c) The variation of (b) β and (c) γ obtained from the fits to the heat capacity measurements for $2 \leq T \leq 5$ K as a function of Au composition. The vertical dotted lines indicate the critical composition ($x_c = 0.3$). In all panels, the values are reported per formula unit.

heat capacity is indeed observed at the critical composition [Fig. 4(a)]. However, it is important to first note that the softening of a single acoustic mode is a small contribution to the heat capacity, which contains contributions from all thermally accessible phonon modes. The critical heat capacity is expected to vary as $\approx T^{2.5}$ [30], which is not dramatically different from the temperature dependence of the noncritical heat capacity ($\approx T^3$). This low contrast in the heat capacity coupled with a small contribution from the soft acoustic mode makes an unambiguous extraction of critical heat capacity difficult. Therefore, the relation $C = \gamma T + \beta T^3$ was utilized to parametrize the low temperature heat capacity in the temperature range of 2–5 K for each composition. Here, the coefficients γ and β represent the electronic and phonon contributions, respectively [60]. As shown in Figs. 4(b) and 4(c), β reaches a maximum value at x_c , while γ remains essentially independent of Au composition. The modest increase in the phonon heat capacity at x_c is in line with the critical softening of the acoustic mode along $\Gamma - X$. Interestingly, β is elevated for compositions larger than x_c , that is, the orthorhombic region of the phase diagram adjacent to the QCP. Measurements that directly probe the unstable acoustic mode would be particularly useful to further illuminate the quantum critical behavior of the elastic QCP.

Recently, the $(\text{Ca}_x\text{Sr}_{1-x})_3\text{Rh}_4\text{Sn}_{13}$ [20,21] and the $(\text{Ca}_x\text{Sr}_{1-x})_3\text{Ir}_4\text{Sn}_{13}$ [22] series have been identified as systems that can be tuned to a displacive SQCP by application of physical or chemical pressure. In an intriguing analogy with many unconventional superconductors, the phase diagrams comprise a dome of superconductivity peaked near a SQCP [21,23,61]. Furthermore, the structural phase transition in these systems occurs with an abrupt change in the Fermi surface associated with a charge density wave [22–26]. Hence, there is a clear distinction with the QCP in $\text{LaCu}_{6-x}\text{Au}_x$ where there is no expectation (or evidence) that electronic degrees of freedom play an important role. Also, an elastic QCP is associated with an instability

of an acoustic mode rather than an optic mode as in the case of a displacive SQCP. Nevertheless, there are some similarities; for example, the phonon specific heat is enhanced near the SQCP in $\text{LaCu}_{6-x}\text{Au}_x$ and somewhat more dramatically in the stannides mentioned above [20,22]. These observations indicate that the elastic QCP studied here is fundamentally different from the displacive SQCP, and the $\text{LaCu}_{6-x}\text{Au}_x$ series appears to be an ideal candidate system to further probe an elastic QCP without the complications of competing electronic phases.

In conclusion, we have studied the $\text{LaCu}_{6-x}\text{Au}_x$ system, where a continuous structural phase transition can be suppressed via Au substitution. A phase diagram showing that the complete suppression of the structural phase transition occurs for $x_c = 0.3$ was constructed from the results of x-ray and neutron diffraction measurements. The low-temperature phonon contribution to the heat capacity rises at the critical composition, indicating residual instability of the orthorhombic structure at low temperature. These observations indicate that the suppression of the monoclinic phase with Au substitution in $\text{LaCu}_{6-x}\text{Au}_x$ likely results in a QCP. DFT calculations support the idea that the QCP in $\text{LaCu}_{6-x}\text{Au}_x$ arises from an elastic instability with no significant involvement of electronic degrees of freedom. Further investigation of $\text{LaCu}_{6-x}\text{Au}_x$ should prove invaluable in the elucidation of the fundamental properties of an elastic QCP.

We acknowledge V. Keppens, V. Fanelli, T. Williams, and P. Whitfield for useful discussions, F. Ye for help with sample characterization, and M. Suchomel for assistance with the synchrotron x-ray measurements. The research at the High Flux Isotope Reactor (ORNL) is supported by the Scientific User Facilities Division, Office of Basic Energy Sciences, U.S. Department of Energy (DOE). Use of the Advanced Photon Source at Argonne National Laboratory was supported by the U.S. Department of Energy, Office of Science, Office of Basic Energy Sciences, under Contract No. DE-AC02-06CH11357. A. F. M., M. A. M., S. M.,

and D. M. acknowledge the support of the U.S. Department of Energy, Office of Science, Basic Energy Sciences, Materials Sciences and Engineering Division. Work at the University of Missouri was supported by DOE through the S3TEC Energy Frontier Research Center Award No. DE-SC0001299/DE-FG02-09ER46577. Work performed at the National High Magnetic Field Laboratory is supported by National Science Foundation (NSF) Cooperative Agreement No. DMR-1157490, the State of Florida, and the U.S. Department of Energy (DOE NNSA DE-NA0001979).

This manuscript has been authored by UT-Battelle, LLC under Contract No. DE-AC05-00OR22725 with the U.S. Department of Energy. The U.S. Government retains a nonexclusive, paid-up, irrevocable, world-wide license to publish or reproduce the published form of this manuscript, or allow others to do so, for U.S. Government purposes. The views and conclusions contained herein are those of the authors and should not be interpreted as necessarily representing the official policies or endorsements, either expressed or implied, of the U.S. Government or any U.S. Government agency.

*lpoudel@vols.utk.edu

- [1] T. Park, F. Ronning, H. Q. Yuan, M. B. Salamon, R. Movshovich, J. L. Sarrao, and J. D. Thompson, *Nature (London)* **440**, 65 (2006).
- [2] S. Nakatsuji, K. Kuga, Y. Machida, T. Tayama, T. Sakakibara, Y. Karaki, H. Ishimoto, S. Yonezawa, Y. Maeno, E. Pearson, G. G. Lonzarich, L. Balicas, H. Lee, and Z. Fisk, *Nat. Phys.* **4**, 603 (2008).
- [3] G. R. Stewart, *Rev. Mod. Phys.* **56**, 755 (1984).
- [4] H. v. Löhneysen, A. Rosch, M. Vojta, and P. Wölfle, *Rev. Mod. Phys.* **79**, 1015 (2007).
- [5] N. D. Mathur, F. M. Grosche, S. R. Julian, I. R. Walker, D. M. Freye, R. K. W. Haselwimmer, and G. G. Lonzarich, *Nature (London)* **394**, 39 (1998).
- [6] S. Sachdev, *Science* **288**, 475 (2000).
- [7] B. Lake, D. A. Tennant, and S. E. Nagler, *Phys. Rev. Lett.* **85**, 832 (2000).
- [8] M. Kenzelmann, Y. Chen, C. Broholm, D. H. Reich, and Y. Qiu, *Phys. Rev. Lett.* **93**, 017204 (2004).
- [9] C. Rüegg, B. Normand, M. Matsumoto, A. Furrer, D. F. McMorrow, K. W. Krämer, H. U. Güdel, S. N. Gvasaliya, H. Mutka, and M. Boehm, *Phys. Rev. Lett.* **100**, 205701 (2008).
- [10] R. Oppermann and H. Thomas, *Z. Phys. B* **22**, 387 (1975).
- [11] R. Folk, H. Iro, and F. Schwabl, *Phys. Rev. B* **20**, 1229 (1979).
- [12] T. Schneider, H. Beck, and E. Stoll, *Phys. Rev. B* **13**, 1123 (1976).
- [13] Y. T. Millev and D. I. Uzunov, *J. Phys. C* **16**, 4107 (1983).
- [14] J. F. Scott, *Rev. Mod. Phys.* **46**, 83 (1974).
- [15] R. Morf, T. Schneider, and E. Stoll, *Phys. Rev. B* **16**, 462 (1977).
- [16] S. E. Rowley, L. J. Spalek, R. P. Smith, M. P. M. Dean, M. Itoh, J. F. Scott, G. G. Lonzarich, and S. S. Saxena, *Nat. Phys.* **10**, 367 (2014).
- [17] K. A. Müller and H. Burkard, *Phys. Rev. B* **19**, 3593 (1979).
- [18] E. L. Venturini, G. A. Samara, M. Itoh, and R. Wang, *Phys. Rev. B* **69**, 184105 (2004).
- [19] S. U. Handunkanda, E. B. Curry, V. Voronov, A. H. Said, G. G. Guzmán-Verrí, R. T. Brierley, P. B. Littlewood, and J. N. Hancock, *Phys. Rev. B* **92**, 134101 (2015).
- [20] S. K. Goh, D. A. Tompsett, P. J. Saines, H. C. Chang, T. Matsumoto, M. Imai, K. Yoshimura, and F. M. Grosche, *Phys. Rev. Lett.* **114**, 097002 (2015).
- [21] W. C. Yu, Y. W. Cheung, P. J. Saines, M. Imai, T. Matsumoto, C. Michioka, K. Yoshimura, and S. K. Goh, *Phys. Rev. Lett.* **115**, 207003 (2015).
- [22] L. E. Klintberg, S. K. Goh, P. L. Alireza, P. J. Saines, D. A. Tompsett, P. W. Logg, J. Yang, B. Chen, K. Yoshimura, and F. M. Grosche, *Phys. Rev. Lett.* **109**, 237008 (2012).
- [23] P. K. Biswas, Z. Guguchia, R. Khasanov, M. Chinotti, L. Li, K. Wang, C. Petrovic, and E. Morenzoni, *Phys. Rev. B* **92**, 195122 (2015).
- [24] C. N. Kuo, C. W. Tseng, C. M. Wang, C. Y. Wang, Y. R. Chen, L. M. Wang, C. F. Lin, K. K. Wu, Y. K. Kuo, and C. S. Lue, *Phys. Rev. B* **91**, 165141 (2015).
- [25] C. N. Kuo, H. F. Liu, C. S. Lue, L. M. Wang, C. C. Chen, and Y. K. Kuo, *Phys. Rev. B* **89**, 094520 (2014).
- [26] A. F. Fang, X. B. Wang, P. Zheng, and N. L. Wang, *Phys. Rev. B* **90**, 035115 (2014).
- [27] C. Fang, H. Yao, W.-F. Tsai, J. P. Hu, and S. A. Kivelson, *Phys. Rev. B* **77**, 224509 (2008).
- [28] C. Xu, M. Müller, and S. Sachdev, *Phys. Rev. B* **78**, 020501 (2008).
- [29] E. Fradkin and S. A. Kivelson, *Science* **327**, 155 (2010).
- [30] M. Zacharias, I. Paul, and M. Garst, *Phys. Rev. Lett.* **115**, 025703 (2015).
- [31] K. Yamada, I. Hirosawa, Y. Noda, Y. Endoh, Y. Ōnuki, and T. Komatsubara, *J. Phys. Soc. Jpn.* **56**, 3553 (1987).
- [32] H. Asano, M. Umino, Y. Ōnuki, T. Komatsubara, F. Izumi, and N. Watanabe, *J. Phys. Soc. Jpn.* **56**, 2245 (1987).
- [33] M. Nakazato, N. Wakabayashi, and Y. Ōnuki, *J. Phys. Soc. Jpn.* **59**, 4004 (1990).
- [34] T. Suzuki, T. Goto, A. Tamaki, T. Fujimura, Y. Ōnuki, and T. Komatsubara, *J. Phys. Soc. Jpn.* **54**, 2367 (1985).
- [35] K. Grube, W. H. Fietz, U. Tutsch, O. Stockert, and H. v. Löhneysen, *Phys. Rev. B* **60**, 11947 (1999).
- [36] A. Schröder, G. Aeppli, R. Coldea, M. Adams, O. Stockert, H. Löhneysen, E. Bucher, R. Ramazashvili, and P. Coleman, *Nature (London)* **407**, 351 (2000).
- [37] A. Schröder, G. Aeppli, E. Bucher, R. Ramazashvili, and P. Coleman, *Phys. Rev. Lett.* **80**, 5623 (1998).
- [38] O. Stockert, H. v. Löhneysen, A. Rosch, N. Pyka, and M. Loewenhaupt, *Phys. Rev. Lett.* **80**, 5627 (1998).
- [39] E. Brück, A. Nowack, N. Hohn, E. Paulus, and A. Freimuth, *Z. Phys. B* **63**, 155 (1986).
- [40] See Supplemental Material at <http://link.aps.org/supplemental/10.1103/PhysRevLett.117.235701> for the details of the structural and thermodynamic properties, and DFT calculations, which includes Refs. [41–44].
- [41] H. Rietveld, *J. Appl. Crystallogr.* **2**, 65 (1969).

- [42] J. Rodríguez-Carvajal, *Physica (Amsterdam)* **192B**, 55 (1993).
- [43] Note the cyclic change of lattice parameters when going from the orthorhombic to monoclinic notations.
- [44] T. Herrmannsdörfer, F. Pobell, J. Sebek, and P. Svoboda, *Physica C (Amsterdam)* **388–389**, 565 (2003).
- [45] M. Ruck, G. Portisch, H. G. Schlager, M. Sieck, and H. v. Löhneysen, *Acta Crystallogr. Sect. B* **49**, 936 (1993).
- [46] L. Poudel *et al.*, *Phys. Rev. B* **92**, 214421 (2015).
- [47] M. A. Carpenter, E. K. Salje, and A. Graeme-Barber, *Eur. J. Mineral.* **10**, 621 (1998).
- [48] Note that the statistical error bar on this extrapolation is very small, ± 0.004 . A more realistic upper bound for the error on x_c is given by the interval between the final two compositions, which is 0.025.
- [49] J. P. Perdew, K. Burke, and M. Ernzerhof, *Phys. Rev. Lett.* **77**, 3865 (1996).
- [50] A. Togo and I. Tanaka, *Scr. Mater.* **108**, 1 (2015).
- [51] P. E. Blöchl, *Phys. Rev. B* **50**, 17953 (1994).
- [52] G. Kresse and D. Joubert, *Phys. Rev. B* **59**, 1758 (1999).
- [53] D. J. Singh and L. Nordstrom, *Planewaves, Pseudopotentials, and the LAPW (M)ethod* (Springer Science & Business Media, New York, 2006).
- [54] P. Blaha, K. Schwarz, G. K. H. Madsen, D. Kvasnicka, and J. Luitz, *WIEN2K, An Augmented Plane Wave + Local Orbitals Program for Calculating Crystal Properties* (Karlheinz Schwarz, Techn. Universität Wien, Austria, 2001).
- [55] I. Pomeranchuk, *Exptl. Theoret. Phys. (U.S.S.R.)* **35**, 524 (1958).
- [56] E. K. Salje, *Annu. Rev. Mater. Res.* **42**, 265 (2012).
- [57] H. Harima, A. Yanase, and A. Hasegawa, *J. Phys. Soc. Jpn.* **59**, 4054 (1990).
- [58] D. C. Johnston, *Adv. Phys.* **59**, 803 (2010).
- [59] G. K. Madsen and D. J. Singh, *Comput. Phys. Commun.* **175**, 67 (2006).
- [60] C. Kittel, *Introduction to Solid State Physics* (Wiley, New York, 2005).
- [61] D. A. Tompsett, *Phys. Rev. B* **89**, 075117 (2014).